



## Abstract

Among meteorological elements, precipitation has a large spatial variability and less observation, particularly in High Mountain Asia, although precipitation in mountains is an important parameter for hydrological circulation. We estimated precipitation contributing to glacier mass at median elevation of glaciers, which is presumed to be at equilibrium-line altitude (ELA) so that mass balance is zero at that elevation, by tuning adjustment parameters of precipitation. We also made comparisons between median elevation of glaciers, including the effect of drifting snow and avalanche, and eliminated those local effects. Then, we could obtain median elevation of glaciers depending only on climate to estimate glacier surface precipitation.

The calculated precipitation contributing to glacier mass can elucidate that glaciers in the arid High Mountain Asia have very less precipitation, while much precipitation contribute to glacier mass in the Hindu Kush, the Himalayas, and the Hengduan Shan due to not only direct precipitation amount but also avalanche nourishment. We classified glaciers in High Mountain Asia into summer-accumulation type and winter-accumulation type using the summer accumulation ratio, and confirmed that summer-accumulation type glaciers have a higher sensitivity than winter-accumulation type glaciers.

## 1 Introduction

Meltwater from glaciers and seasonal snow in the high mountains is a significant water resource in Asia (Immerzeel et al., 2010, 2013; Kaser et al., 2010). However, Asian mountains have a poor network of precipitation measurement (Bookhagen and Burbank, 2006), even though precipitation is a crucial parameter for understanding hydrological processes. In addition, meteorological stations in mountain regions are generally located at lower elevations in the valleys, and thus are not representative of basin-scale precipitation because of strong orographic effects.

## Climate regime of Asian glaciers revealed by GAMDAM Glacier Inventory

A. Sakai et al.

Title Page

Abstract

Introduction

Conclusions

References

Tables

Figures



Back

Close

Full Screen / Esc

Printer-friendly Version

Interactive Discussion



Several gridded datasets compiling precipitation have been produced based on ground rain-gauge data or satellite data on a global scale (Chen et al., 2002; New et al., 2000; Huffman et al., 1997). Almost dataset, however, do not consider orographic effects (Adam et al., 2006).

5 Yatagai et al. (2009, 2012) provided the Asian Precipitation – Highly Resolved Observational Data Integration Towards Evaluation of Water Resources (APHRODITE) gridded precipitation dataset based on gauge data from 1951 to 2007. They interpolated precipitation in mountain regions by considering orographic effects on precipitation based on the parameter-elevation regressions on independent slopes model (Daly et al., 1994). The gridded datasets, however, have significant biases against point observational data in the Himalayan mountains (Fujita and Sakai, 2014).

Observed precipitation data at high altitude (Putkonen, 2004) is very rare in the High Mountain Asia. Then, Maussion et al. (2014) have generated a new high-resolution atmospheric dataset, High Asia Reanalysis (HAR) using Weather Research and Forecasting (WRF) model from October 2000 to September 2011. The HAR reproduced well previously reported spatial pattern and seasonality of precipitation. They proposed a new classification based on precipitation seasonality, further, they found glaciers of varying types over very short distances in the Himalayan ranges.

15 Braithwaite and Raper (2002) indicated that calibrated precipitation at equilibrium-line altitude (ELA) (Braithwaite and Zhang, 1999) using the degree-day model was considerably greater than the grid precipitation in New et al. (1999) in New Zealand, the Caucasus, the Alps, southern Norway, northern Scandinavia, Svalbard, and Axel Heiberg Island. Engelhart et al. (2012) calculated spatial distribution of glacier mass balances using gridded temperature and precipitation, and then compared the calculated distribution with observed spatial distribution. They indicated that the gridded precipitation did not represent orographic enhancement of precipitation. Rupper and Roe (2008) estimated ELA by the energy mass balance model, with the NCEP/NCAR reanalysis data at High Mountain Asia, assuming all precipitation as solid. However, the estimated ELA has a large discrepancy with glacier distribution. They noted that

Climate regime of Asian glaciers revealed by GAMDAM Glacier Inventory

A. Sakai et al.

Title Page

Abstract

Introduction

Conclusions

References

Tables

Figures



Back

Close

Full Screen / Esc

Printer-friendly Version

Interactive Discussion



## Climate regime of Asian glaciers revealed by GAMDAM Glacier Inventory

A. Sakai et al.

Title Page

Abstract

Introduction

Conclusions

References

Tables

Figures

◀

▶

◀

▶

Back

Close

Full Screen / Esc

Printer-friendly Version

Interactive Discussion



the reanalysis temperature was a valuable estimator of summer balance, but the reanalysis precipitation was a poor estimator of winter balance. Rasmussen (2013) also pointed out that correlation between the NCEP/NCAR reanalysis precipitation values and winter balance was low. Braithwaite et al. (2006) estimated accumulation at ELA of 180 glaciers using the degree-day model, in which the modelled annual accumulation represented the observed winter balance well. Immerzeel et al. (2012) estimated detail distribution of precipitation on the Karakoram glaciers by assuming a neutral glacier mass balance.

Overall, precipitation in the gridded data still required calibration to calculate glacier mass balance, because amount and seasonality of precipitation strongly affect the sensitivity of glacier mass balance (Oerlemans and Fortuin, 1992; Braithwaite and Raper, 2002; Fujita, 2008).

The objective of this study was to estimate precipitation at the ELA over Asian glaciers derived from the Glacier Area Mapping for Discharge in Asian Mountains (GAMDAM) Glacier Inventory (GGI) (Nuimura et al., 2014), and to evaluate the climate regime at the Asian glaciers. We confirmed that median elevation of glaciers can be proxy data for ELA in the Asian glaciers, and established a method for calculating precipitation at median elevation of glaciers by applying a glacier mass balance model with reanalysis dataset, so that mass balance would be zero, by tuning annual precipitation.

## 2 Study region, data, and method

### 2.1 Study region

Our study region covers High Mountain Asia (26.5–55.5° N, 66.5–104.5° E), which corresponds to the regions of Central Asia, South Asia West, South Asia East, and Altay and Sayan of North Asia in the Randolph Glacier Inventory (Pfeffer et al., 2014) (Fig. 1). The center of our target region have wide Tibetan Plateau, which elevation is around

## Climate regime of Asian glaciers revealed by GAMDAM Glacier Inventory

A. Sakai et al.

Title Page

Abstract

Introduction

Conclusions

References

Tables

Figures

◀

▶

◀

▶

Back

Close

Full Screen / Esc

Printer-friendly Version

Interactive Discussion



5000 m a.s.l. The plateau forms an orographic obstacle for westerlies and Indian monsoons. Indian monsoon supply high amounts of precipitation over the Himalaya, but most moisture is orographically forced out at elevations less than 4000 m a.s.l. and the high altitude glacier area are significantly more arid (Hamper and Humphrey, 2003).

5 Monsoon moisture influence decrease from east to west along the Himalaya, and westerlies moisture becomes important in the West Himalaya and the Karakoram. The moisture boundary between monsoon and westerly lies at 78° E near the Sutlej Valley (Bookhagen and Burbank, 2010). Westerlies can reach higher elevation than the summer monsoon, which may be related to the higher tropospheric extent of the westerly airflow (Scherler et al., 2011). Precipitation increase with altitude and maximum precipitation occur between 5000 and 6000 m a.s.l. (Wake, 1989; Young and Schmok, 1989; Young and Hewitt, 1990; Hewitt, 2011).

15 The Pamir Mountains locate at transition zone influenced by the monsoon and the westerlies. Those eastern part: the climate characterised as semiarid and arid mountain climate because surrounded by high mountains (Hindu Kush, Alay, Tien Shan, and Karakoram Mountains) (Zech et al., 2005).

20 The Tien Shan range constitutes the first montane barrier for northern and western air masses travelling from Siberia and the Kazakh steppes to Central Asia. The resulting barrier effects lead to a distinct continentality gradient with decreasing precipitation rates. Sorg et al. (2012) summarized that Western and Northern Tien Shan can be classified to moist region, and Central Tien Shan and Eastern Tien Shan have continental arid/semiarid climate. In terms of the seasonality of precipitation, maximum precipitation occur winter in Western Tien Shan, spring and early summer in Northern and Eastern Tien Shan, and summer in Central Tien Shan.

25 In the Altai range, one of the main factors that determines the climatic regime is interaction between the Siberian High and western cyclonic activity (Surazakov et al., 2007). Aizen et al. (2006a) reported that two-thirds of accumulation was come from oceanic (Atlantic or Arctic) and the rest was recycled over Aral-Caspian sources in the Russian Altai mountains.

## Climate regime of Asian glaciers revealed by GAMDAM Glacier Inventory

A. Sakai et al.

Title Page

Abstract

Introduction

Conclusions

References

Tables

Figures

◀

▶

◀

▶

Back

Close

Full Screen / Esc

Printer-friendly Version

Interactive Discussion



Sayan range locates north-western edge of Mongolia, arid/semiarid region. Precipitation in Mongolia is supplied by the synoptic-scale disturbances during the summer (June–August) because this region in the westerly dominant zone. the regions contributing to precipitation in Mongolia are western Siberia located to the northwest of Mongolia (Sato et al., 2007).

Thus, most precipitation source at inland of the High Mountain Asia are originated continental recycled evaporation, and such high ratio of continental recycling cannot find in the other continents (Yoshimura et al., 2004).

These circulation systems characterize the glaciers as summer-accumulation type and winter-accumulation type (Ageta and Higuchi, 1984; Fujita and Ageta, 2000).

Most glaciers in the Himalayas (Bolch et al., 2012) or on the Tibetan Plateau (Yao et al., 2012) are shrinking and also in Tien Shan (Aizen et al., 2006b) and Altai (Surazakov et al., 2007), while glaciers in the Karakoram and Pamir is in the state of slight mass gain (Gardelle et al., 2013). Further, recent analyses Kääb et al. (2012) and Gardner et al. (2013) elucidated that the glacier fluctuations have contrasting behaviours in Asia by comparing digital elevation models between ICESat (Ice, Cloud, and land Elevation Satellite) and the SRTM (Shuttle Radar Topography Mission). Fujita and Nuimura (2011) also indicated that the fluctuation of glaciers in High Mountain Asia were spatially heterogeneous, based on calculated ELA with reanalysis datasets.

### 2.2 Median elevation and ELA derived from GGI

The GGI is a quality controlled glacier outline based on the Landsat level 1 terrain corrected (L1T) scenes, which was delineated manually (Nuimura et al., 2014). Because systematic geometric corrections are performed for the L1T products, the GGI can provide precise hypsometry of glaciers.

ELA is defined as the elevation of zero mass balance. Several researchers have proposed different methods for estimating ELA, such as the shape of contour lines and the accumulation area ratio (AAR) method (Torsnes et al., 1993; Benn and Lehmkuhl, 2000; Carrivick and Brewer, 2004). Braithwaite and Raper (2009) demonstrated the

## Climate regime of Asian glaciers revealed by GAMDAM Glacier Inventory

A. Sakai et al.

Title Page

Abstract

Introduction

Conclusions

References

Tables

Figures

◀

▶

◀

▶

Back

Close

Full Screen / Esc

Printer-friendly Version

Interactive Discussion



median elevation of 94 glaciers in the World Glacier Inventory (WGI), each with balanced-budget ELA, which is the elevation of zero mass balance for a particular glacier. They showed that median elevations of glaciers (where elevation divides glacier area equally) are available for balanced-budget ELA. Paul et al. (2002) (Swiss Alps), Rastner et al. (2012) (Greenland), Racoviteanu et al. (2008) (Cordillera Blanca in Peru) also show median elevations at each region as an indicator of ELA. In the GLIMS glacier inventory, median elevation is one of an important basic parameter derived by compiling the glacier polygon data and Digital Elevation Model (Paul et al., 2009).

We compared observed ELA with median elevation derived from each GGI (Nuimura et al., 2014) using ASTER GDEM (ver. 2) (Table S1). Figure 2 indicates that decadal ELAs are consistent with the median elevation of each glacier (rmse = 83; bias = +11), whereas annual ELAs vary widely (rmse = 119).

Nuimura et al. (2014) also indicated that distribution of the snow line altitude of glaciers in China reported by Shi (2008) also corresponded well with median elevation of glaciers derived from the GGI.

### 2.3 Median elevation of glaciers as proxy data for ELA

Drifting snow has a significant contribution to glacier accumulation and affects the present glacier distributions (Jaedicke and Gauer, 2005). Avalanche snow from ice-free slopes is also an important source of glacier accumulation in precipitous terrains (Benn and Lehmkuhl, 2000; Hewitt, 2014). Thus, ELA and median elevation of glaciers are affected not only by temperature and precipitation but also by those alternative sources of glacier nourishment.

Here, we set three median elevation of glaciers: G-median elevation, L-median elevation, and W-median elevation. We calculate median elevation of glaciers at each  $0.5^\circ \times 0.5^\circ$  grid by area-weighted average.

### 2.3.1 G-median elevation

We calculate median glacier elevation, area-weighted average at each  $0.5^\circ$  grid using GGI in High Mountain Asia. The minimum glacier area is  $0.05 \text{ km}^2$  (Nuimura et al., 2014). Here, we define the simple median glacier elevation as G-median elevation.

### 2.3.2 L-median elevation

Some median elevations of glaciers averaged at each grid reflect only a few small glaciers. Small glaciers in undulating terrain have been under strong influence of drifting snow and cannot maintain snow or ice mass without drifting snow. Those small glaciers can exist at much lower altitudes than large glaciers. Therefore, we analysed the representativeness of each median elevation of glaciers and the glaciers using GGI.

Median anomaly is the difference between median elevation of each glacier and the average median elevation of the vicinity glaciers. The vicinity glaciers were defined as glaciers locate inside the  $0.5^\circ \times 0.5^\circ$  grid, with the centre on the location of the glacier, which is defined at the centre of gravity of each glacier. Figure 3a shows that glaciers with a smaller area have large variability of median anomaly. Here, we selected those glaciers with more than 300 glaciers in the vicinity ( $0.5^\circ \times 0.5^\circ$  grid). In particular, glaciers smaller than  $1 \text{ km}^2$  in area have large standard deviations ( $\text{STDV} > 230 \text{ (m)}$ ) of the median anomaly, and the number of outliers ( $2\sigma$ ) is more than 18 000, whereas glaciers larger than  $1 \text{ km}^2$  have less than 300 outliers (Fig. 3b). This means that smaller glaciers are affected by local terrain.

Dahl and Nesje (1992) reported that ELA depression of cirque glaciers is caused by leeward accumulation. Conversely, the windy side of cirque glaciers tend to have higher ELA because of denudation of deposited snow. Further, small glaciers with high median anomalies might be separated glaciers from ablation areas, and those with low median anomalies might be composed of drift snow accumulated by depression. Those with large anomalies of median elevation can be explained by re-distribution of snow because of wind effect or topography.

Then, G-median elevations of glaciers are affected by local terrain, in particular, at the grid with only small glaciers. Here, we propose a median elevation, L-median elevation, which is calculated by excluding glaciers smaller than  $1 \text{ km}^2$  in area.

### 2.3.3 W-median elevation

Each median elevation of glaciers is sometimes affected by the geography surrounding the glacier. Scherler et al. (2011) reported that avalanche-fed glaciers have a lower median elevation against snow line elevation in the Himalayas. Steep avalanche walls, at which snow cannot be retained at the surface, were excluded from the GGI (Nuimura et al., 2014). The median elevation of avalanche-fed glaciers would be lowered by the amount of avalanche snow accumulation, which should accumulate at the steep avalanche wall. Then, median elevation of avalanche-fed glaciers calculated from area-altitude distribution, including glaciers as well as steep avalanche walls, would reflect ELA depending only on temperature and precipitation (not affected by avalanche nourishment). Sensitivity of glacier mass balance to temperature change requires ice or snow mass accumulating on the glacier including not only direct precipitation, but also avalanche nourishment. The glacier mass balance, however, usually is calculated from only direct precipitation as an input meteorological data. Therefore, the relation between direct precipitation and ice or snow mass accumulating on the glacier is significant for calculation for glacier mass fluctuation. To estimate direct precipitation on glaciers, we tried to estimate median elevations of glaciers, including steep avalanche walls. Figure S1 shows an example of the estimation of median elevations of glaciers, including steep avalanche walls. We assumed that hypsometry of steep avalanche walls can be estimated by linear interpolation between the area at the altitude of maximum glacier area and maximum ground altitude, at which area is assumed to be zero. Then, median elevation of glaciers, including avalanche walls became 6125 m (W-median) from 5394 m (L-median). Here, we define the elevation as W-median elevation. If calculated, W-median elevation is lower than L-median elevation and equal to L-median elevation.

## Climate regime of Asian glaciers revealed by GAMDAM Glacier Inventory

A. Sakai et al.

Title Page

Abstract

Introduction

Conclusions

References

Tables

Figures



Back

Close

Full Screen / Esc

Printer-friendly Version

Interactive Discussion



## 2.4 Meteorological data

Daily NCEP/NCAR reanalysis data (Kalnay et al., 1996), including temperature (level), geopotential height (level), surface wind (surface flux 10 m), surface humidity (surface), and solar radiation (surface flux), from 1952 to 2007 were used to calculate glacier mass balance. Daily temperatures are given at each median elevation of glaciers, where lapse rate of air temperature is estimated by the temperature at two geopotential heights interleaving the median elevation. Daily precipitation data, APHRODITE from 1952 to 2007, were also used to calculate glacier mass balance.

## 2.5 Glacier mass balance model

The glacier mass balance model, based on the heat balance method provided by Fujita and Ageta, (2000), Fujita et al. (2007); and Fujita et al. (2011), was used to calculate mass balance at median elevations (G-, L-, and W-median elevations), which are the area-weighted average at each  $0.5^\circ \times 0.5^\circ$  grid. The mass balance model, based on the daily heat balance, required air temperature, relative humidity, wind speed, solar radiation, and precipitation, and mass balance consisting of snow accumulation, melt, refreezing, and evaporation. Longwave radiation was calculated by application of the equation established by Kondo (1990) using dew point temperature at the screen height and a coefficient related to the sunshine ratio (ratio of downward shortwave radiation to solar radiation at the top of the atmosphere). This mass balance model also takes into account refreezing amounts from ice temperature change. Calculation interval was daily.

First, we calculated the mass balance at each median elevation using APHRODITE and reanalysis NCEP/NCAR data from 1952 to 1978, assuming that the initial values of ice temperature and snow depth are  $0^\circ$  and 0.1 m, respectively. Then, we could obtain initial condition values of ice temperature and snow depth for subsequent mass balance calculations from 1979 to 2007. To calculate optimized precipitation at median elevations, we calculated, assuming that mass balance from 1979 to 2007 should be

equal to zero by adjusting the APHRDITE precipitation data as shown in Fig. 4.

$$P_{\text{cal}} = A_p \times P_{\text{ap}}, \quad (1)$$

where  $A_p$  is the adjusting ratio of APHRDITE precipitation and  $A_p$  is constant for each grid.

The phase of precipitation, solid (snow) ( $C_a$ , positive sign) or liquid (rain), depending on air temperature, is important for glacier mass balance. Precipitation ( $P_p$ ) is separated solid and liquid by temperature, assuming the occurrence probability of solid precipitation. The following relation between the probability of snowfall and air temperature was obtained from data observed by Fujita and Nuimura (2011) on the Tibetan Plateau:

$$C_a = \begin{cases} P_p & [T_a \leq 0] \text{ (}^\circ\text{C)} \\ \left(1 - \frac{T_a}{4}\right) P_p & [0 < T_a < 4] \text{ (}^\circ\text{C)} \\ 0 & [T_a \geq 4] \text{ (}^\circ\text{C)} \end{cases} \quad (2)$$

### 3 Results

#### 3.1 Distribution of median elevations of glaciers

Figure 5 shows the distribution of three types of median elevations of glaciers (G-, L-, W-median elevations). They are area-weighted means at each  $0.5^\circ \times 0.5^\circ$  grid. There are 943 grids in G-median elevations, and L- and W-median elevations have 671 grids. Figure 5a compares distribution of G-median elevations at the eastern Sayan Mountains, in the west of the Altai Mountains, at the Qilian Mountains, and in the east of Hengduan Shan (see location in Fig. 1), excluding glaciers smaller than  $1 \text{ km}^2$  in area.

Distribution of the difference between W-median elevation and L-median elevation (Fig. S2) indicates that the Tibetan Plateau has less difference. The Kalakoram, the

Himalayas, and the Hengduan Shan have relatively large differences, which reflects that glaciers in these regions are surrounded by steep avalanche walls at the upper part. The relation between G- and L-median elevations (Fig. S3) indicates that median elevations changed both positively and negatively by eliminating small size glaciers ( $< 1 \text{ km}^2$ ).

In contrast, median elevation of glaciers shift to higher altitude by taking into account steep avalanche walls, which are depicted by the relation between G- and W-median elevations. Further, the change of median elevation of glaciers between G- and L-median is much larger than that between G- and W-median.

### 3.2 Precipitation contributing to mass balance at ELA

Figure 6 shows that annual precipitation of APHRODITE and calculated precipitations at median elevation derived from the G-, L-, W-median elevations (Fig. 5). Here these calculated precipitations, which contribute to glacier mass at the G-, L-, W-median elevations, are indicated by  $P_G$ ,  $P_L$ , and  $P_W$ , respectively. Little precipitation around the Taklimakan Desert and much precipitation at the Hengduan Shan and the southern edge of the Himalayas and the Karakoram were found. These calculated precipitations at ELA reflect regional climate in High Mountain Asia. However, several grids have extraordinarily large amounts of precipitation in the eastern Sayan Mountains, the west of the Altai Mountains, the southern edge of Himalayas, and the Hengduan Shan (Fig. 6b). Although,  $P_L$  in Fig. 6c in several grids at the Hengduan Shan, the southern edge of the Himalayas, and the Karakoram was still extremely large, those grids have less  $P_W$  in Fig. 6d. Figure S4 shows ratio of  $P_L$  to  $P_W$ . For example, the ratio of 2.0 implies that avalanche nourishment contribution is as same as the amount of direct precipitation. Ratio more than two is found at high relief terrains such as the Central, East Himalayas and the Hengduan Shan, the Karakoram and the Pamir. Then, large amount of avalanche nourishment would contribute to the glacier mass in those regions.

## Climate regime of Asian glaciers revealed by GAMDAM Glacier Inventory

A. Sakai et al.

Title Page

Abstract

Introduction

Conclusions

References

Tables

Figures

◀

▶

◀

▶

Back

Close

Full Screen / Esc

Printer-friendly Version

Interactive Discussion



Still, there are several grids that have extremely large precipitation compared with adjacent grids. Those overestimations would be caused by missed glacier delineation or unreasonable estimation of the steep avalanche wall.

The  $T-P$  plot (relation between summer (JJA) temperature and annual  $P_L$  with error are shown in Fig. S5). The details of the  $T-P$  plot are discussed in Sect. 4.2.1. Root mean square error was 83 m between decadal average of ELA and median elevation of each glacier (Fig. 2). Then, both vertical and horizontal error bars were calculated assuming that L-median elevation has  $\pm 83$  m error.

### 3.3 Validation

Although direct observation of precipitation at ELA are scarce, winter balance was observed at several glaciers in High Mountain Asia, which was compiled by Dyurgerov (2002) (Table S3). We compared the calculated snow amount based on G-, L-, and W-median elevations with the observed winter balance from 1997 to 2000 at corresponding grids (Fig. 7). APHRODITE snow was calculated by use of daily temperature at each ELA based on Eq. (2). The figure shows APHRODITE snow is significantly less than the observed winter accumulation. Further, snow amount derived from G-, L-, and W-median elevations tend to be smaller than the winter balance, but the correlation coefficient is statistically significant and much higher than that with APHRODITE snow.

Accumulated snow at the end of winter is reported as “winter balance” in the report of Dyurgerov (2002). The highest correlation coefficient between average observed winter balance and accumulation calculated on the basis of L-median elevation are obtained, although the correlation coefficient between observed winter balance and calculated precipitation based on W-median elevation was low. The reason behind this might be the fact that observed winter balance includes not only surface precipitation but also avalanche nourishment during winter. Then, observed winter balance can be a validation for accumulation during winter, including drifting snow and avalanche. However, it cannot be a validation for direct precipitation during winter.

## Climate regime of Asian glaciers revealed by GAMDAM Glacier Inventory

A. Sakai et al.

Title Page

Abstract

Introduction

Conclusions

References

Tables

Figures

⏪

⏩

◀

▶

Back

Close

Full Screen / Esc

Printer-friendly Version

Interactive Discussion



## 4 Discussion

### 4.1 Input meteorological data

Fujita and Ageta (2000) concluded that the air temperature and solar radiation are the major elements for calculation of glacier ablation. Hence, accuracy of calculated precipitation at median elevations of glaciers depends on the accuracy of air temperature and solar radiation. We therefore compared daily reanalysis data of air temperature and solar radiation with those observed data, which were measured on or adjacent to glaciers. Analysed site names, locations, and observed periods are summarized in Table S2.

Figure S6a shows that reanalysis temperature data corresponded well, in particular high temperature (during melting season). Meanwhile, solar radiation of reanalysis data is less than observed data, especially in the summer time (Fig. S6b). NCEP/NCAR cannot reproduce well during cloudy days (not shown) in the glacier area and reanalysis of downward solar radiation on cloudy days is higher than that of observed data. Then, the overestimation of solar radiation would cause overestimation of the calculated precipitation at the median elevation of glaciers, particularly in Indian monsoon affected regions (the Himalayas and Hengduan Shan).

### 4.2 Climate on median elevation of glaciers

#### 4.2.1 Relation between temperature and precipitation at median elevation

Several researchers have analysed the relation between summer (JJA) temperature and annual precipitation at ELA ( $T-P$  plot) and discussed climatology of glaciers (e.g., Nesje and Dahl, 2000). Ohmura et al. (1992) established the relation between summer (JJA) temperature and annual precipitation at ELA ( $T-P$  plot) for 70 glaciers in the world. Braithwaite et al. (2006) also discussed the effect of vertical lapse rate for temperature based on the observed winter balance and model annual temperature sum of

180 glaciers in the world.  $T-P$  plots can show the climate regime of glaciers, and the slope of the  $T-P$  can indicate the sensitivity of glaciers to temperature change (Ohmura et al., 1992).

The  $T-P$  plot in Fig. 8 indicates that APHRODITE precipitation cannot represent the relation reported by Ohmura et al. (1992). We also depict  $T-P$  plots at G-, L-, W-median elevations at each grid in Fig. 8.  $T-P$  plot of G-median elevation includes high temperature range (5–10°C). The reason for this is that G-median elevation reflects the elevation of small glaciers composed by drifting snow at several tens of grids.  $T-P$  plot of L-median elevations contain very large precipitation at the 3–5°C temperature range, because glacier mass is affected by avalanche, particularly in the Hengduan Shan, the Himalayas, and the Karakoram. Those fitted curves of G and L have larger inclination than Ohmura's equation at the high temperature range. On the other hand, the fitted curve of the  $T-P$  plot based on W-median elevation corresponds well with Ohmura's equation, which implies that calculated precipitation based on W-median elevation represents reasonable results.

#### 4.2.2 Accumulation season and $T-P$ plot

Fujita (2008) has reported that summer-accumulation type glaciers (SAG) have higher sensitivity at ELA under the idealized meteorological variables. Hengduan Shan, Bhutan, Everest, and West Nepal are strongly influenced by the Indian and South-east Asian summer monsoons, and glaciers are SAG. On the other hand, the climate at Pamir, Hindu Kush, and Karakoram are dominated by the westerlies, and glaciers are winter-accumulation type glaciers (WAG) (Gardelle et al., 2013). Himachal Pradesh and Jammu Kashmir (included in the W Himalaya in Fig. 1) are transition zones, influenced by both the monsoon and the westerlies (Bookhagen and Burbank, 2010). We can classify glaciers into SAG and WAG using the 40% summer (JJA) precipitation ratio (SPR) to annual precipitation (APHRODITE from 1979 to 2007) in High Mountain Asia, as shown in Fig. 9.

## Climate regime of Asian glaciers revealed by GAMDAM Glacier Inventory

A. Sakai et al.

Title Page

Abstract

Introduction

Conclusions

References

Tables

Figures

◀

▶

◀

▶

Back

Close

Full Screen / Esc

Printer-friendly Version

Interactive Discussion



## Climate regime of Asian glaciers revealed by GAMDAM Glacier Inventory

A. Sakai et al.

Title Page

Abstract

Introduction

Conclusions

References

Tables

Figures

◀

▶

◀

▶

Back

Close

Full Screen / Esc

Printer-friendly Version

Interactive Discussion



Sensitivity of the glacier mass can be evaluated by the gradient of the relation between JJA temperature and annual precipitation at ELA ( $T-P$  plot), according to Ohmura et al. (1992). Figure 10 shows the  $T-P$  plot reported by Ohmura et al. (1992) based on 70 glaciers in the world and calculated at each grid in High Mountain Asia at W-median elevations, which are classified into WAG and SAG. SAG have higher sensitivity than Ohmura's equation, particularly in the high temperature regions. WAG have slightly less but similar sensitivity with Ohmura's equation. The reason for this is that Ohmura et al. (1992) established the  $P-T$  plot based mainly on WAG.

Plots of SAG have wider variations against the fitted curve than those of WAG (Fig. 10), which reflects that SAG have a wider range distribution in latitude (in other words, wider range of summer radiation, Ohmura et al., 1992) than that of WAG (Fig. 10).

Braithwaite et al. (2006) also depict the  $T-P$  plot based on 180 glaciers, and indicate that Arctic glaciers have low (less than  $0^{\circ}$ ) temperature and less precipitation. Figure 10 also indicates that there are glaciers with less precipitation and low temperature in High Mountain Asia, and those glaciers have less sensitivity to temperature change because high Asian mountains contain glaciers in inland arid regions. Thus, High Mountain Asia can retain the ice mass stably, like glaciers in the Arctic.

### 4.3 Adjustment ratio of precipitation: $A_p$

Figure 11 shows the distribution of  $A_p$  (adjustment ratio of APHRODITE data), calculated based on W-median elevation. Although, W-median elevation at most grids is higher than the elevation in the grid average (including glacier-free zones), the eastern Himalayas, the central Himalayas, Pamir, and central Tien Shan have adjustment ratios of less than 1, implying that the APHRODITE precipitation data overestimate the precipitation at median elevation of glaciers.

We compared the altitudinal distributions of grid numbers for the median elevation of glaciers and the mean altitude of each grid in the Himalayas and the Karakoram (Fig. S7a, b). Both modes of median elevation of glaciers and mean altitude of grids

## Climate regime of Asian glaciers revealed by GAMDAM Glacier Inventory

A. Sakai et al.

Title Page

Abstract

Introduction

Conclusions

References

Tables

Figures

◀

▶

◀

▶

Back

Close

Full Screen / Esc

Printer-friendly Version

Interactive Discussion



show equal altitude (5000 m a.s.l. and 5500 m a.s.l., respectively). On the other hand, in the Himalayan region, several researchers reported that maximum precipitation occurs at 3000 m elevation (Burbank et al., 2003; Putkonen, 2004; Bookhagen and Burbank, 2006), which is lower than the W-median elevation of glaciers (Fig. S7a). Then, the calculated precipitation at the median elevation of glaciers would be less than the grid average precipitation, which is also affected by larger precipitation at lower elevation because precipitation gauges are usually set at low elevation. Hence, the mode of  $A_p$  is less than 1 (Fig. S7c). Fujita and Nuimura (2011) and Fujita and Sakai (2014) also reported that observed precipitation at Tsho Rolpa in the east Nepal Himalayas (27.9° N, 86.5° E) was less than the APHRODITE precipitation data.

In the Karakoram region, the mode of  $A_p$  is approximately 1 (1.0–1.2) (Fig. S7c). The reason is that glaciers in the Karakoram have almost the same altitudinal distribution of W-median glacier elevation and average ground altitude, at which the altitude of peak precipitation (5000–6000 m a.s.l.) corresponded (Wake, 1989; Young and Schmok, 1989; Young and Hewitt, 1990; Hewitt, 2011).

Yatagai et al. (2012) compared the APHRODITE with the Global Precipitation Climatology Centre (GPCC) product, which is also compiled gauge precipitation data. Distribution of the difference (APHRODITE-GPCC) (Fig. 9a of Yatagai et al., 2012) indicates that APHRODITE estimates less precipitation than the GPCC product in most areas. APHRODITE data, however, were larger than the GPCC product only around the central Tien Shan and Pamir regions. Then, those regions have the adjustment ratio of less than 1.

## 5 Conclusion

We calculated precipitation contributing to glacier mass at median elevation of glaciers, which can be proxy data of ELA, using a glacier mass balance model by adjusting precipitation data. Three types of median elevations of glaciers are proposed. They are (1) G-median elevation, which is calculated to include small glaciers ( $< \text{km}^2$ ), (2) L-

median elevation, which eliminates small glaciers, and (3) W-median elevation, which is calculated to include steep avalanche walls. L-median elevation eliminated local terrain effects, such as drifting snow, which was included in G-median elevation. W-median elevation depends only on climate and excludes the effect of avalanche nourishment.

Precipitation estimated based on G- and L-median elevation have extremely large values at several tens of grids, and those fitted curves of  $T-P$  plots have large gradients. In contrast, distribution of precipitation calculated based on W-median elevation does not have grids with extremely large amounts of precipitation, because the W-median glacier elevation depends only on climate and is not affected by avalanche nourishment.

Estimated precipitation at W-median elevations elucidated the  $T-P$  conditions of glaciers in High Mountain Asia. Glaciers in High Mountain Asia are located in low temperature zones, such as glaciers in the Arctic. Further, it was elucidated that glaciers in high relief terrains (such as the Central, East Himalayas and the Hengduan Shan, the Karakoram and the Pamir) tend to have large amount of avalanche nourish contribution to the glacier mass by comparing  $P_L$  (including avalanche nourishment) and  $P_W$  (only direct precipitation).

We differentiated summer-accumulation type glaciers and winter-accumulation type glaciers using the 40 % summer precipitation ratio to annual precipitation. Fitted curves of winter-accumulation type glaciers corresponded well with Ohmura's equation. However, the curves of summer-accumulation type glaciers have higher gradients, particularly at larger precipitation ranges, which indicate that summer-accumulation type glaciers have higher sensitivity to climate change.

$A_p$  values were less than 1 at the western, central, and eastern Himalayas, and approximately 1 at Karakoram. The reason for this is the altitudinal relation between the median elevation of glaciers and the precipitation gradient.

**The Supplement related to this article is available online at  
doi:10.5194/tcd-8-3629-2014-supplement.**

**Climate regime of  
Asian glaciers  
revealed by GAMDAM  
Glacier Inventory**

A. Sakai et al.

Title Page

Abstract

Introduction

Conclusions

References

Tables

Figures



Back

Close

Full Screen / Esc

Printer-friendly Version

Interactive Discussion



*Acknowledgements.* This research was supported by the Funding Program for Next Generation World-Leading Researchers (NEXT Program). We express our sincere thanks and appreciation for great support to Y. Hoshina, S. Tsutaki, K. Tsunematu, S. Omiya, S. Okamoto, K. Taniguchi, and P. Tshering.

## References

- Adam, J. C., Clark, E. A., Lettenmaier, D. P., and Wood, E. F.: Correction of global precipitation products for orographic effects, *J. Climate*, 19, 15–38, 2006.
- Aizen, V. B., Aizen, E. M., Joswiak, D. R., Fujita, K., Takeuchi, N., and Nikitin, S. A.: Climatic and atmospheric circulation pattern variability from ice-core isotope/geochemistry records (Altai, Tien Shan and Tibet), *Ann. Glaciol.*, 43, 49–60, 2006a.
- Aizen, V. B., Kuzmichenok, V. A., Surazakov, A. B., and Aizen, E. M.: Glacier changes in the central and northern Tien Shan during the last 140 years based on surface and remote-sensing data, *Ann. Glaciol.*, 43, 202–213, 2006b.
- Ageta, Y. and Higuchi, K.: Estimation of mass balance components of summer-accumulation type glacier in the Nepal Himalaya, *Geogr. Ann.*, 66, 249–255, 1984.
- Benn, I. D. and Lehmkuhl, F.: Mass balance and equilibrium-line altitudes of glaciers in high-mountain environments, *Quatern. Int.*, 65/66, 15–29, 2000.
- Bolch, T., Kulkarni, A., Kääb, A., Huggel, C., Paul, F., Cogley, J. G., Frey, H., Kargel, J. S., Fujita, K., Scheel, M., Bajracharya, S., and Stoffel, M.: The state and fate of Himalayan glaciers, *Science*, 336, 310–314, doi:10.1126/science.1215828, 2012.
- Bookhagen, B. and Burbank, D. W.: Topography, relief, and TRMM-derived rainfall variations along the Himalaya, *Geophys. Res. Lett.*, 33, L08405, doi:10.1029/2006GL026037, 2006.
- Bookhagen, B. and Burbank, D.: Toward a complete Himalayan hydrological budget: spatiotemporal distribution of snowmelt and rainfall and their impact on river discharge, *J. Geophys. Res.*, 115, F03019, doi:10.1029/2009JF001426, 2010.
- Braithwaite, R. J. and Raper, S. C. B.: Glaciers and their contribution to sea level change, *Phys. Chem. Earth*, 27, 1445–1454, 2002.
- Braithwaite, R. J. and Raper, S. C. B.: Estimating equilibrium-line altitude (ELA) from glacier inventory data, *Ann. Glaciol.*, 53, 127–132, 2009.

## Climate regime of Asian glaciers revealed by GAMDAM Glacier Inventory

A. Sakai et al.

Title Page

Abstract

Introduction

Conclusions

References

Tables

Figures

◀

▶

◀

▶

Back

Close

Full Screen / Esc

Printer-friendly Version

Interactive Discussion





---

## Climate regime of Asian glaciers revealed by GAMDAM Glacier Inventory

A. Sakai et al.

---

Title Page

Abstract

Introduction

Conclusions

References

Tables

Figures



Back

Close

Full Screen / Esc

Printer-friendly Version

Interactive Discussion



- Fujita, K., Seko, K., Ageta, Y., Pu, J. C., and Yao, T. D.: Superimposed ice in glacier mass balance on the Tibetan Plateau, *J. Glaciol.*, 42, 454–460, 1996.
- Fujita, K., Ageta, Y., Pu, J., and Yao, T.: Mass balance of Xiao Dongkemadi Glacier on the central Tibetan Plateau from 1989 to 1995, *Ann. Glaciol.*, 31, 159–163, 2000.
- 5 Fujita, K., Ohta, T., and Ageta, Y.: Characteristics and climatic sensitivities of runoff from a cold-type glacier on the Tibetan Plateau, *Hydrol. Process.*, 21, 2882–2891, doi:10.1002/hyp.6505, 2007.
- Fujita, K., Takeuchi, N., Nikitin, S. A., Surazakov, A. B., Okamoto, S., Aizen, V. B., and Kubota, J.: Favorable climatic regime for maintaining the present-day geometry of the Gregoriev  
10 Glacier, Inner Tien Shan, *The Cryosphere*, 5, 539–549, doi:10.5194/tc-5-539-2011, 2011.
- Gardelle, J., Berthier, E., Arnaud, Y., and Käab, A.: Region-wide glacier mass balances over the Pamir-Karakoram-Himalaya during 1999–2011, *The Cryosphere*, 7, 1263–1286, doi:10.5194/tc-7-1263-2013, 2013.
- 15 Gardner, A. S., Moholdt, G., Cogley, J. G., Wouters, B., Arendt, A. A., Wahr, J., Berthier, E., Hock, R., Pfeffer, W. T., Kaser, G., Ligtenberg, S. R. M., Bolch, T., Sharp, M. J., Hagen, J. O., van den Broeke, M. R., and Paul, F.: A reconciled estimate of glacier contributions to sea level rise: 2003 to 2009, *Science*, 340, 852–857, doi:10.1126/science.1234532, 2013.
- Harper, J. T. and Humphrey, N.: High altitude Himalayan climate inferred from glacial ice flux, *Geophys. Res. Lett.*, 30, 1764, doi:10.1029/2003GL017329, 2003.
- 20 Hewitt, K.: Glacier change, concentration, and elevation effects in the Karakoram Himalaya, Upper Indus Basin, *Mt. Res. Dev.*, 31, 188–200, 2011.
- Hewitt, K.: *Glaciers of the Karakoram Himalaya*, Springer, 363 pp., the Netherlands, 2014.
- Huffman, G. J., Adler, R. F., Arkin, P., Chang, A., Ferraro, R., Gruber, A., Janowiak, J., and McNab, A.: The Global Precipitation Climatology Project (GPCP) combined precipitation  
25 dataset, *B. Am. Meteorol. Soc.*, 78, 5–20, 1997.
- Immerzeel, W. W., Ludovicus, P. H. B., and Bierkens, M. F. P.: Climate change will affect the Asian water towers, *Science*, 328, 1382–1385, doi:10.1126/science.1183188, 2010.
- Immerzeel, W. W., Pellicciotti, F., and Shrestha, A. B.: Glaciers as a proxy to quantify the spatial distribution of precipitation in the Hunza Basin, *Mt. Res. Dev.*, 32, 30–38, 2012.
- 30 Immerzeel, W. W., Pellicciotti, F., and Bierkens, M. F. P.: Rising river flows throughout the twenty-first century in two Himalayan glacierized watersheds, *Nat. Geosci.*, 6, 742–745, doi:10.1038/NGEO1896, 2013.



---

## Climate regime of Asian glaciers revealed by GAMDAM Glacier Inventory

A. Sakai et al.

---

Title Page

Abstract

Introduction

Conclusions

References

Tables

Figures

◀

▶

◀

▶

Back

Close

Full Screen / Esc

Printer-friendly Version

Interactive Discussion



- Paul, F., Barry, R. G., Cogley, J. G., Frey, H., Haeberli, W., Ohmura, A., Ommanney, C. S. L., Raup, B., Rivera, A., and Zemp, M.: Recommendations for the compilation of glacier inventory data from digital sources, *Ann. Glaciol.*, 50, 119–126, 2009.
- 5 Pfeffer, W. T., Arendt, A. A., Bliss, A., Bolch, T., Cogley, J. G., Gardner, A. S., Hagen, J. O., Hock, R., Kaser, G., Kienholz, C., Miles, E. S., Moholdt, G., Mölg, N., Paul, F., Radiæ, V., Rastner, P., Raup, B. H., Rich, J., and Sharp, M. J.: The Randolph consortium: the Randolph Glacier Inventory: a globally complete inventory of glaciers, *J. Glaciol.*, 60, 537–552, 2014.
- Putkonen, J. K.: Continuous snow and rain data at 500 to 4400 m altitude near Annapurna, Nepal, 1991–2001, *Arct. Antarct. Alp. Res.*, 36, 244–248, 2004.
- 10 Racoviteanu, A. E., Arnaud, Y., Williams, M. W., and Ordonez, J.: Decadal changes in glacier parameters in the Cordillera Blanca, Peru, derived from remote sensing, *J. Glaciol.*, 54, 499–510, 2008.
- Rasmussen, L. A.: Meteorological controls on glacier mass balance in High Asia, *Ann. Glaciol.*, 54, 352–359, doi:10.3189/2013AoG63A353, 2013.
- 15 Rastner, P., Bolch, T., Mölg, N., Machguth, H., Le Bris, R., and Paul, F.: The first complete inventory of the local glaciers and ice caps on Greenland, *The Cryosphere*, 6, 1483–1495, doi:10.5194/tc-6-1483-2012, 2012.
- Rupper, S. and Roe, G.: Glacier changes and regional climate: a mass and energy balance approach, *J. Climate*, 21, 5384–5401, doi:10.1175/2008JCLI2219.1, 2008.
- 20 Sato, T., Tsujimura, M., Yamanaka, T., Iwasaki, H., Sugimoto, A., Sugita, M., Kimura, F., Davaa, G., and Oyunbaatar, D.: Water sources in semiarid northeast Asia as revealed by field observations and isotope transport model, *J. Geophys. Res.*, 112, D17112, doi:10.1029/2006JD008321, 2007.
- Scherler, D., Bookhagen, B., and Strecker, M. R.: Hillslope glacier coupling: the interplay of topography and glacial dynamics in High Asia, *J. Geophys. Res.*, 116, F02019, doi:10.1029/2010JF001751, 2011.
- 25 Shi, Y. (Ed.): *Concise Glacier Inventory of China*, Shanghai Popular Science Press, China, Shanghai, 2008.
- Sorg, A., Bolch, T., Stoffel, M., Solomina, O., and Beniston, M.: Climate change impacts on glaciers and runoff in Tien Shan (Central Asia), *Nature Clim. Change*, 2, 725–731, doi:10.1038/NCLIMATE1592, 2012.
- 30

## Climate regime of Asian glaciers revealed by GAMDAM Glacier Inventory

A. Sakai et al.

Title Page

Abstract

Introduction

Conclusions

References

Tables

Figures



Back

Close

Full Screen / Esc

Printer-friendly Version

Interactive Discussion



Surazakov, A. B., Aizen, V. B., Aizen, E. M., and Nikitin, S. A.: Glacier changes in the Siberian Altai Mountains, Ob river basin, (1952–2006) estimated with high resolution imagery, *Environ. Res. Lett.*, 2, 045017, doi:10.1088/1748-9326/2/4/045017, 2007.

Torsnes, I., Rye, N., and Nesje, A.: Modern and Little Ice Age equilibrium-line altitudes on outlet valley glaciers from Jostedalbreen, Norway: an evaluation of different approaches to their calculation, *Arctic Alpine Res.*, 25, 106–116, 1993.

Wake, C. P.: Glaciochemical investigations as a tool to determine the spatial variation of snow accumulation in the Central Karakoram, Northern Pakistan, *Ann. Glaciol.*, 13, 279–284, 1989.

Yao, T., Thompson, L., Yang, W., Yu, W., Gao, Y., Guo, X., Yang, X., Duan, K., Zhao, H., Xu, B., Pu, J., Lu, A., Xiang, Y., Kattel, D. B., and Joswiak, D.: Different glacier status with atmospheric circulations in Tibetan Plateau and surroundings, *Nature Clim. Change*, 2, 663–667, doi:10.1038/nclimate1580, 2012.

Yatagai, A. O., Arakawa, K., Kamiguchi, H., Kawamoto, M., Nodzu, I., and Hamada, A.: A 44-year daily gridded precipitation dataset for Asia based on a dense network of rain gauges, *SOLA*, 5, 137–140, doi:10.2151/sola.2009-035, 2009.

Yatagai, A., Kamiguchi, K., Arakawa, O., Hamada, A., Yasutomi, N., and Kitoh, A.: APHRODITE: constructing a long-term daily gridded precipitation dataset for Asia based on a dense network of rain gauges, *B. Am. Meteorol. Soc.*, 93, 1401–1415, doi:10.1175/BAMS-D-11-00122.1, 2012.

Yoshimura, K., Oki, T., Ohte, N., and Kanae, S.: Colored Moisture Analysis Estimates of Variations in 1998 Asian Monsoon Water Sources, *J. Meteorol. Soc. Jpn.*, 82, 1315–1329, 2004.

Young, G. J. and Hewitt, K.: Hydrological Research in the upper Indus basin, Karakoram Himalaya, Pakistan, *IAHS-AISH P.*, 190, 139–152, 1990.

Young, G. J. and Schmok, J. P.: Ice loss in the ablation area of a Himalayan glacier: studies on Miari Glacier, Karakoram Mountains, Pakistan, *Ann. Glaciol.*, 13, 289–293, 1989.

Zech, R., Abramowski, U., Glaser, B., Sosin, P., Kubik, P. W., and Zech, W.: Late Quaternary glacial and climate history of the Pamir Mountains derived from cosmogenic  $^{10}\text{Be}$  exposure ages, *Quaternary Res.*, 64, 212–220, 2005.

## Climate regime of Asian glaciers revealed by GAMDAM Glacier Inventory

A. Sakai et al.

Title Page

Abstract

Introduction

Conclusions

References

Tables

Figures



Back

Close

Full Screen / Esc

Printer-friendly Version

Interactive Discussion

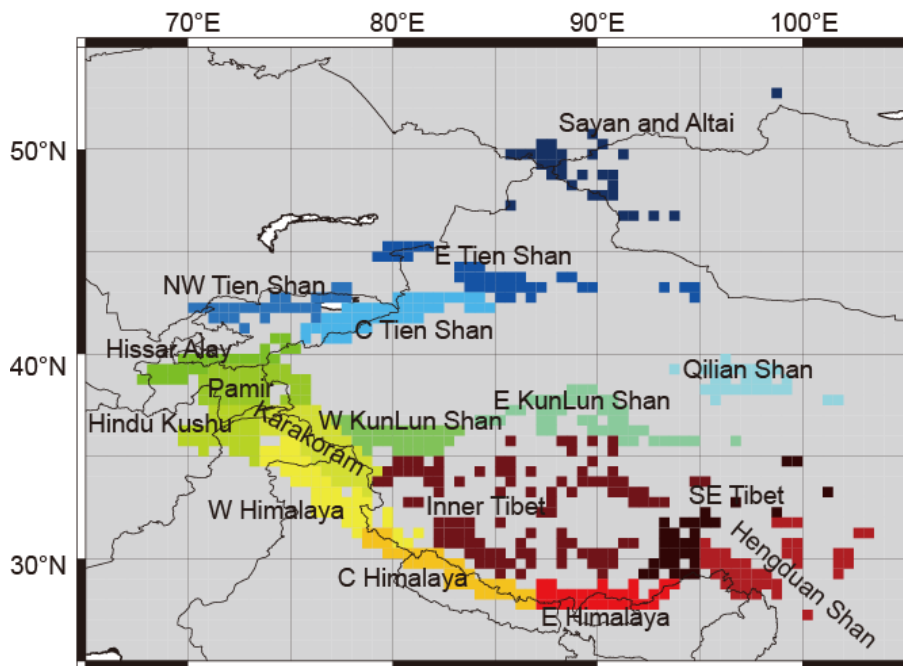


**Figure 1.** Region name and location of grid where the GGI occupied.

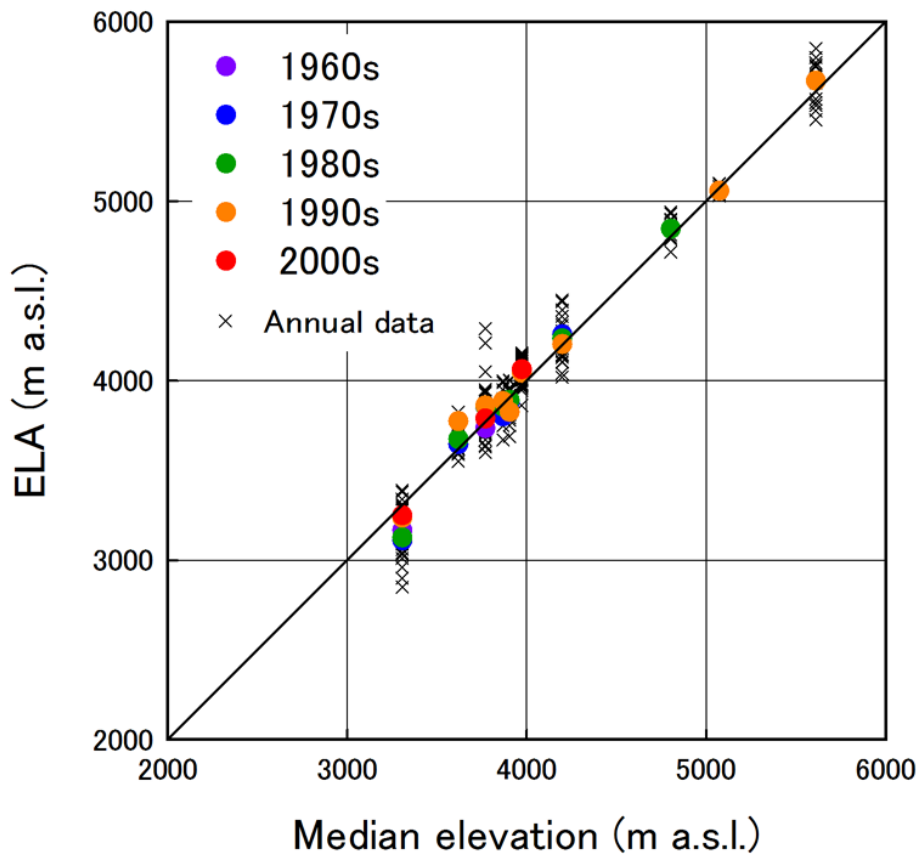


**Figure 2.** Relation between median elevation derived from the GGI and annual observed ELAs.

Title Page

Abstract Introduction

Conclusions References

Tables Figures

◀ ▶

◀ ▶

Back Close

Full Screen / Esc

Printer-friendly Version

Interactive Discussion



## Climate regime of Asian glaciers revealed by GAMDAM Glacier Inventory

A. Sakai et al.

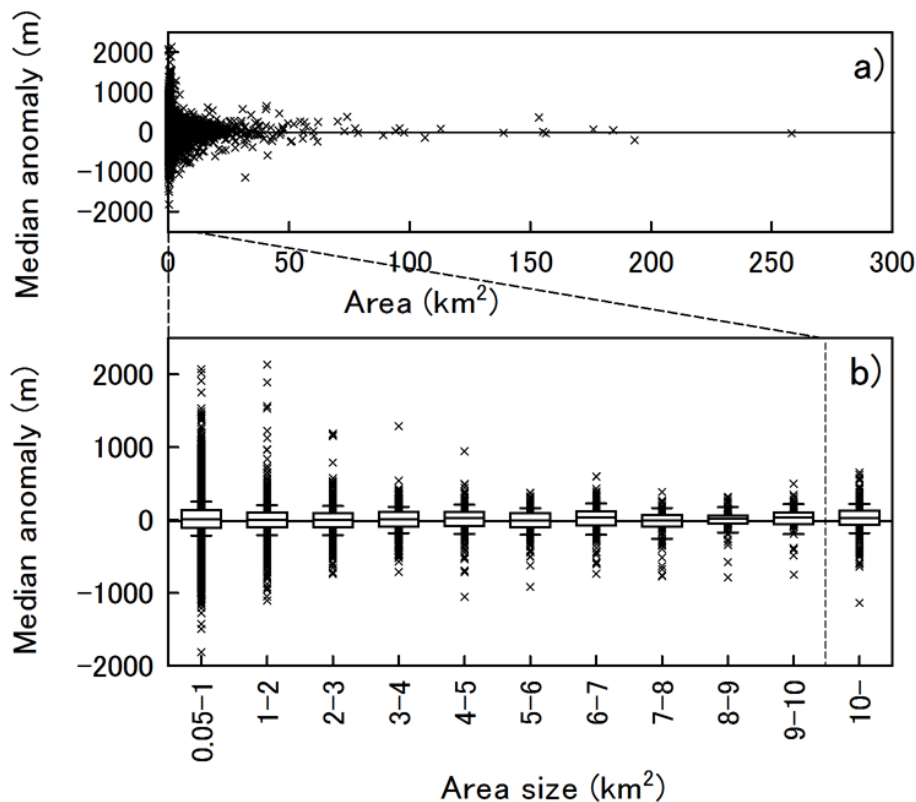


**Figure 3.** (a) Relation between glacier area and median anomaly, which glaciers have more than 300 vicinity glaciers (within  $0.5^\circ \times 0.5^\circ$  grid). (b) Median anomaly distribution in  $1 \text{ km}^2$  bins up to  $10 \text{ km}^2$ . Boxes give lower and upper quartiles of median glacier altitude in  $1 \text{ km}^2$  bin. Vertical error bars indicate standard deviation of data range. Crosses lie outside of this range.

Title Page

Abstract

Introduction

Conclusions

References

Tables

Figures

◀

▶

◀

▶

Back

Close

Full Screen / Esc

Printer-friendly Version

Interactive Discussion



## Climate regime of Asian glaciers revealed by GAMDAM Glacier Inventory

A. Sakai et al.

Title Page

Abstract

Introduction

Conclusions

References

Tables

Figures

◀

▶

◀

▶

Back

Close

Full Screen / Esc

Printer-friendly Version

Interactive Discussion

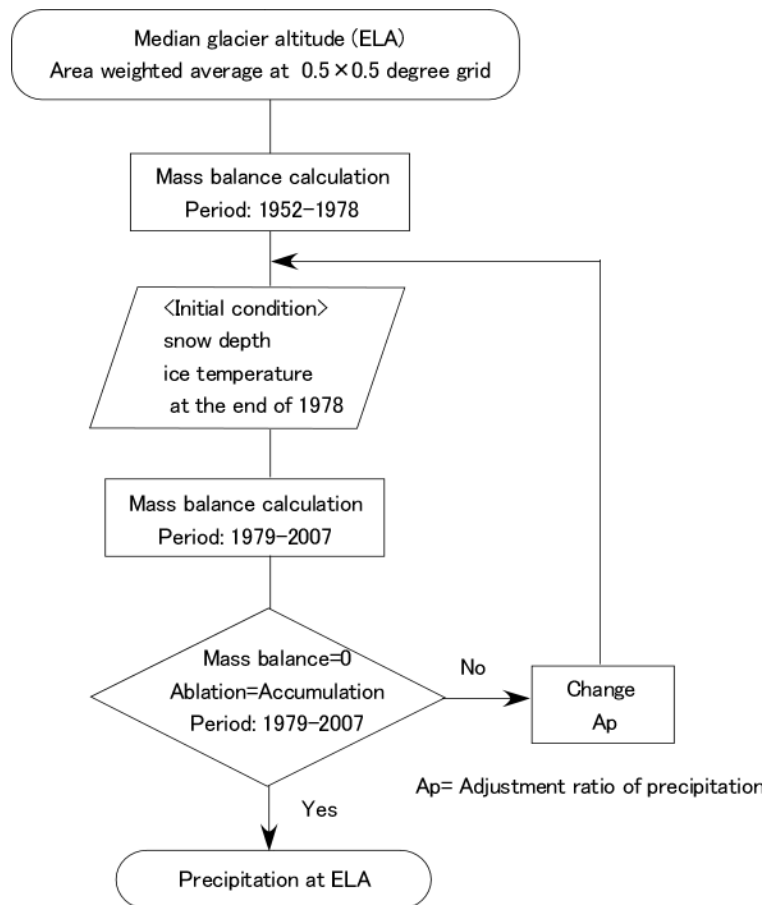


**Figure 4.** Flowchart of calculation of precipitation at median altitude.

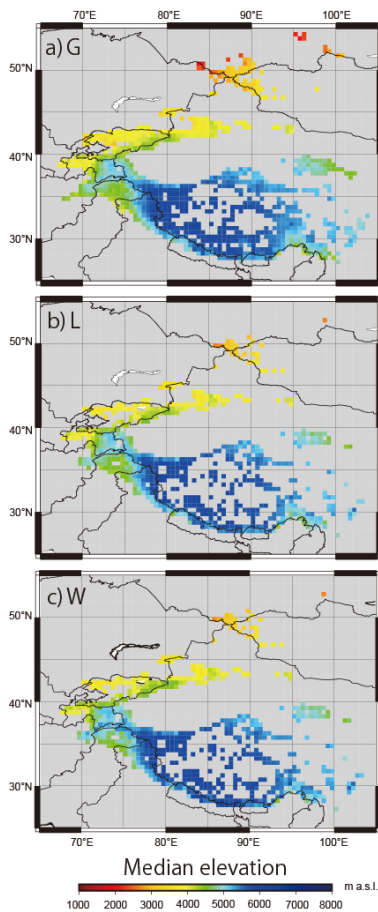


**Figure 5.** Distributions of (a) G-, (b) L-, and (c) W-median elevation. These distributions are the area-weighted average at each 0.5° grid.

Climate regime of Asian glaciers revealed by GAMDAM Glacier Inventory

A. Sakai et al.

Title Page	
Abstract	Introduction
Conclusions	References
Tables	Figures
◀	▶
◀	▶
Back	Close
Full Screen / Esc	
Printer-friendly Version	
Interactive Discussion	



## Climate regime of Asian glaciers revealed by GAMDAM Glacier Inventory

A. Sakai et al.

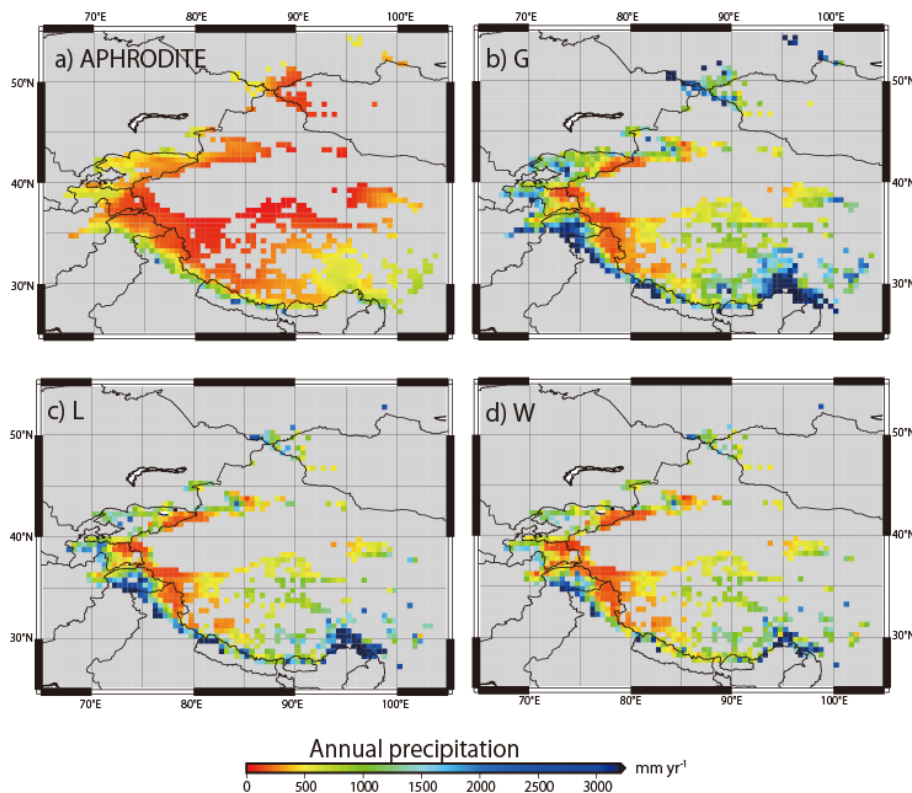


**Figure 6.** Annual precipitation of APHRODITE averaged from 1979 to 2007 (a), at which glacier located in the GGI. Calculated annual precipitation assumed to accumulate on glacier surfaces based on (b) G-, (c) L-, and (d) W-median elevations.

[Title Page](#)[Abstract](#)[Introduction](#)[Conclusions](#)[References](#)[Tables](#)[Figures](#)[◀](#)[▶](#)[◀](#)[▶](#)[Back](#)[Close](#)[Full Screen / Esc](#)[Printer-friendly Version](#)[Interactive Discussion](#)

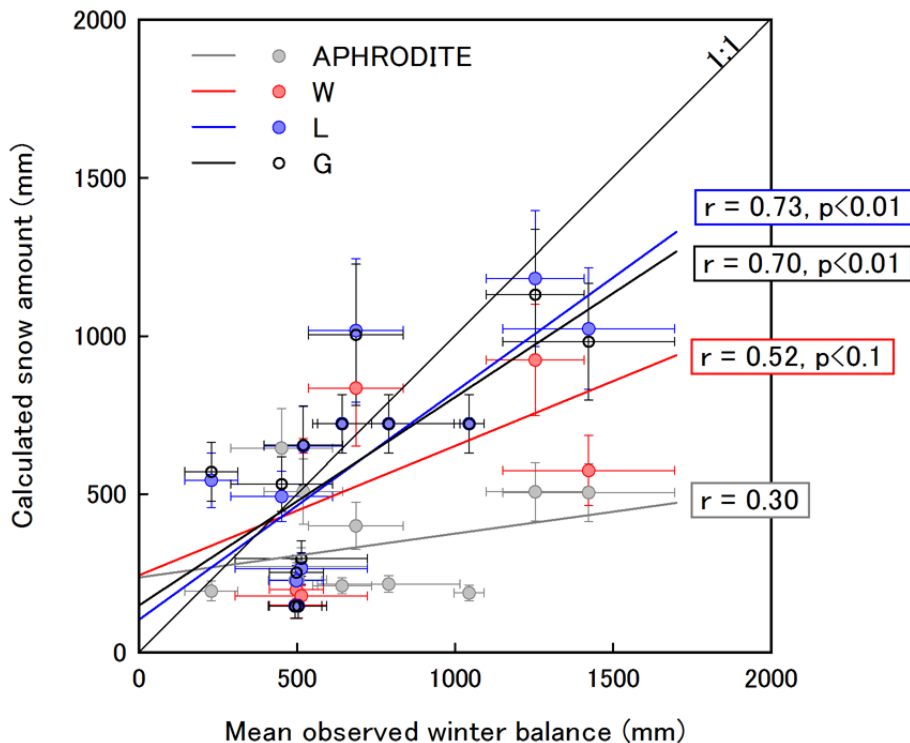


**Figure 7.** Relation between observed winter balance averaged from 1979 to 2000 and calculated snow amounts. Grey circles indicate the snow amounts calculated from APHRODITE. Hollow small circles, blue circles, and red circles show those snow amounts calculated from precipitation based on G-median elevation, L-median elevation, and W-median elevation, respectively. Both vertical and horizontal error bars indicate standard deviation of each annual value.

Climate regime of Asian glaciers revealed by GAMDAM Glacier Inventory

A. Sakai et al.

Title Page

Abstract Introduction

Conclusions References

Tables Figures

◀ ▶

◀ ▶

Back Close

Full Screen / Esc

Printer-friendly Version

Interactive Discussion



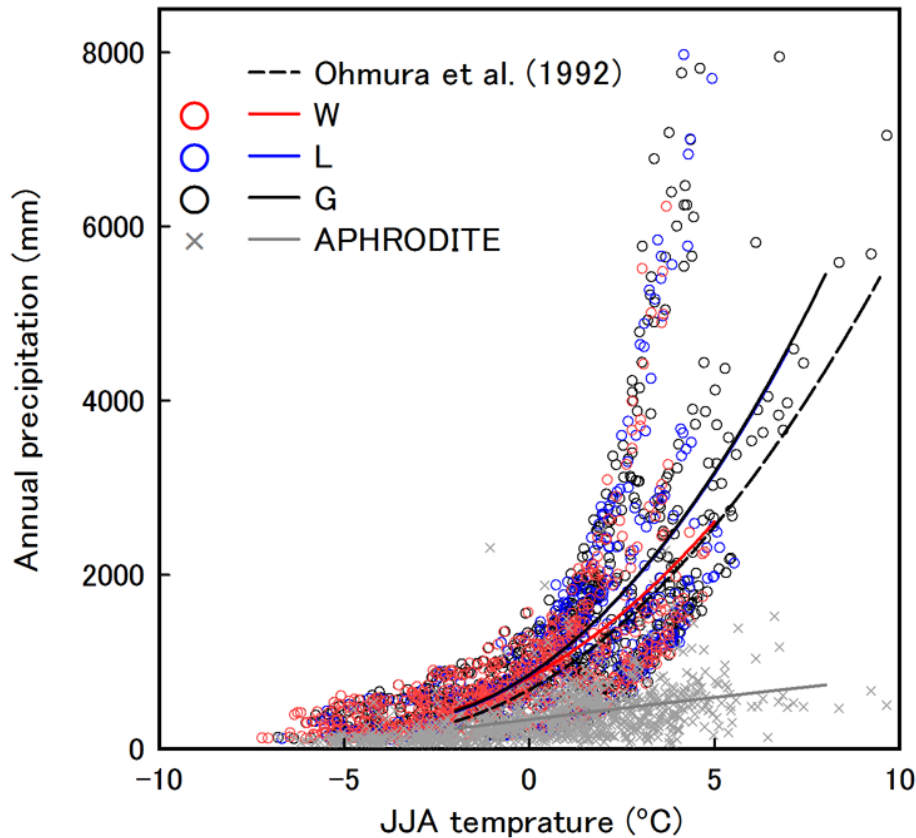


**Figure 8.** Relation between summer (JJA) temperature and annual precipitation at G-median (black circles) L-median (blue circles) W-median (red circles) elevations and APHRODITE averaged from 1979 to 2007 (grey crosses). Fitted curves of each dataset are plotted and shown by the respective colour. The fitted curve derived by Ohmura et al. (1992) is shown by the black dashed line.

Climate regime of Asian glaciers revealed by GAMDAM Glacier Inventory

A. Sakai et al.

Title Page	
Abstract	Introduction
Conclusions	References
Tables	Figures
◀	▶
◀	▶
Back	Close
Full Screen / Esc	
Printer-friendly Version	
Interactive Discussion	



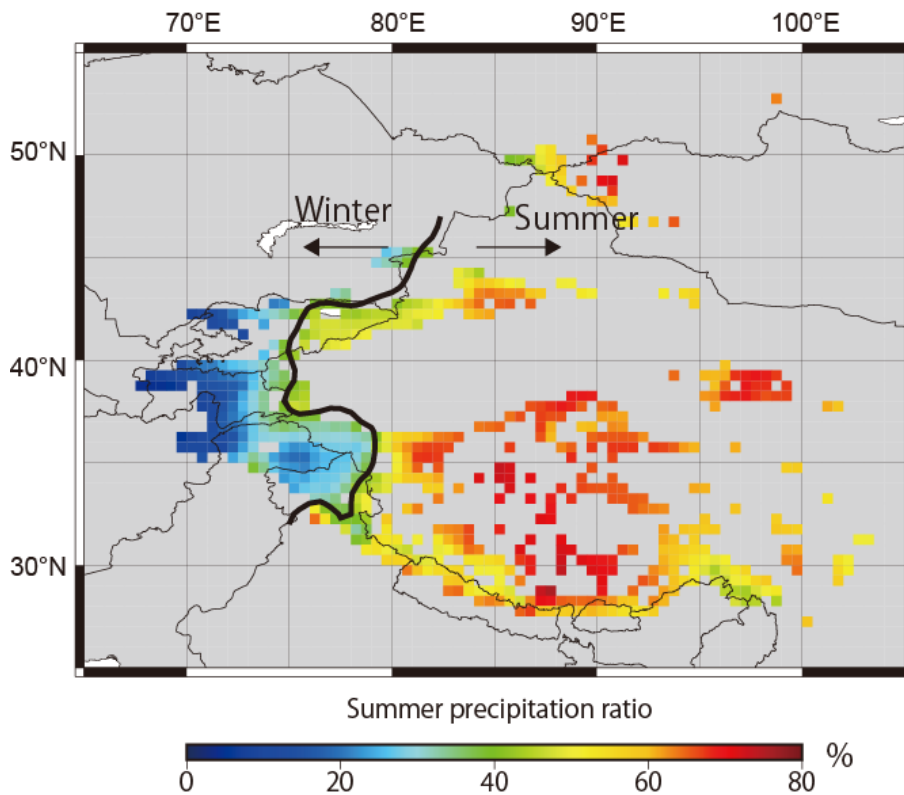


**Figure 9.** Distribution of summer precipitation ratio to annual precipitation. Black thick line indicates the contour of the 40% summer precipitation ratio.

Climate regime of Asian glaciers revealed by GAMDAM Glacier Inventory

A. Sakai et al.

Title Page

Abstract Introduction

Conclusions References

Tables Figures

◀ ▶

◀ ▶

Back Close

Full Screen / Esc

Printer-friendly Version

Interactive Discussion



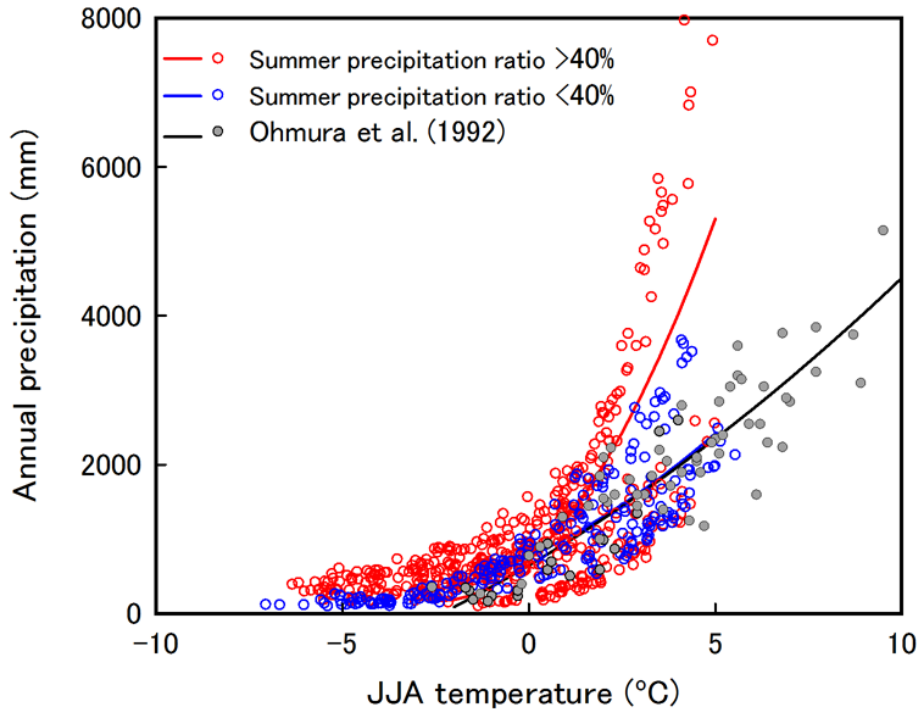


**Figure 10.** Relation between mean summer (JJA) air temperature and annual precipitation at L-median elevation. Red and blue circles indicate summer-accumulation type and winter-accumulation type glaciers, respectively. Grey circles indicate the dataset reported by Ohmura et al. (1992).

**Climate regime of Asian glaciers revealed by GAMDAM Glacier Inventory**

A. Sakai et al.

Title Page	
Abstract	Introduction
Conclusions	References
Tables	Figures
◀	▶
◀	▶
Back	Close
Full Screen / Esc	
Printer-friendly Version	
Interactive Discussion	



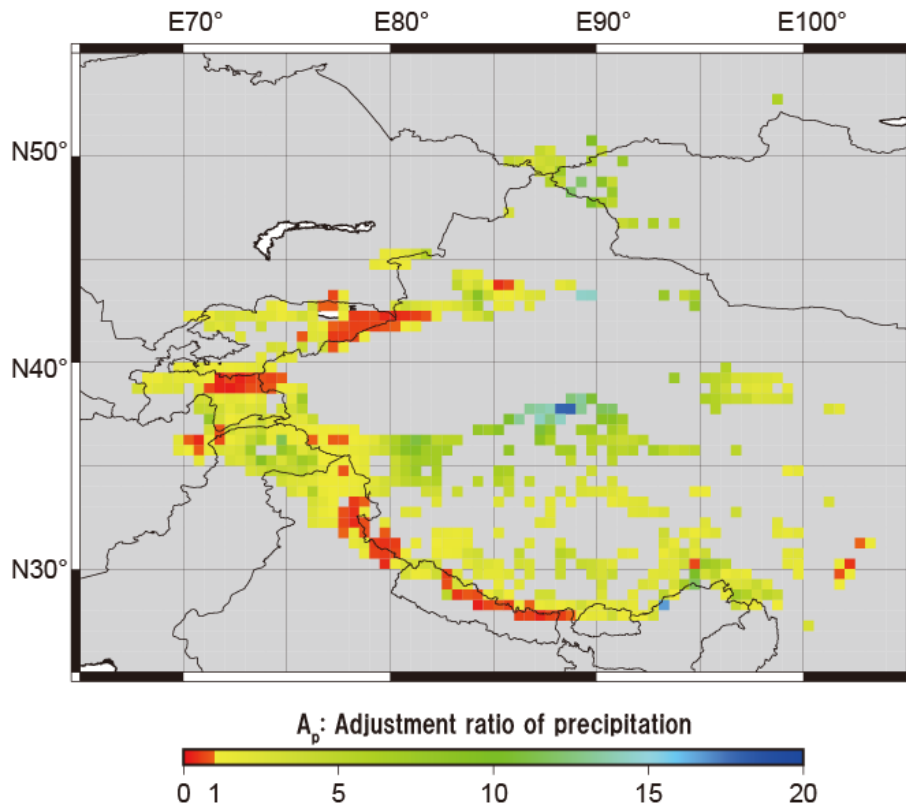


**Figure 11.** Distribution of the adjustment ratio of  $P_W$  to APHRODITE precipitation at each  $0.5^\circ$  grid. Grids with adjustment ratio of less than one are indicated by red.

**Climate regime of Asian glaciers revealed by GAM DAM Glacier Inventory**

A. Sakai et al.

Title Page	
Abstract	Introduction
Conclusions	References
Tables	Figures
◀	▶
◀	▶
Back	Close
Full Screen / Esc	
Printer-friendly Version	
Interactive Discussion	

